J Mol Model (2014) 20:2189
DOI 10.1007/s00894-014-2189-5

ORIGINAL PAPER

Implementing electrostatic polarization cannot fill the gap between experimental and theoretical measurements for the ultrafast fluorescence decay of myoglobin

Bingbing Lin · Ya Gao · Yongxiu Li · John Z. H. Zhang · Ye Mei

Received: 28 December 2013 / Accepted: 24 February 2014

Abstract Over the past few years, time-dependent ultrafast fluorescence spectroscopy method has been applied to the study of protein dynamics. However, observations from these experiments are in a controversy with other experimental studies. Participating of theoretical methods in this debate has not reconciled the contradiction, because the predicted initial relaxation from computer simulations is one-order faster than the ultrafast fluorescence spectroscopy experiment. In those simulations, pairwise force fields are employed, which have been shown to underestimate the roughness of the free energy landscape. Therefore, the relaxation rate of protein and water molecules under pairwise force fields is falsely exaggerated. In this work, we compared the relaxations of tryptophan/environment interaction under linear response approximation employing pairwise, polarized, and polarizable force fields. Results show that although the relaxation can be slowed down to a certain extent, the large gap between experiment and theory still cannot be filled.

Keywords Electrostatic polarization · Myoglobin · Ultrafast fluorescence decay

B. Lin · Y. Gao · Y. Li · J. Z. H. Zhang · Y. Mei (✉)
Center for Laser and Computational Biophysics, State Key Laboratory of Precision Spectroscopy, East China Normal University, Shanghai 200062, China
e-mail: ymei@phy.ecnu.edu.cn

J. Z. H. Zhang · Y. Mei
Department of Physics, Institute of Theoretical and Computational Science, East China Normal University, Shanghai 200062, China

J. Z. H. Zhang · Y. Mei
NYU-ECNU Center for Computational Chemistry at NYU Shanghai, Shanghai, China 200062

Introduction

Water is an integral part of most proteins. Thermal motion of hydration waters, also known as biological waters, shows strong heterogeneity controlled by the topography and the electrostatic property of protein surface, which differentiates them from bulk waters. Understanding the hydration dynamics of biological systems is essential to many biological processes such as protein hydration, protein folding [1–9]. Local order and mobility of water molecules around protein correlate well with the variability of protein structure [10–12]. In return, the three-dimensional structures and dynamics of proteins are slaved by water molecules in the hydration layer. Water molecule serves as lubricant for large conformational changes of proteins as in folding and realization of enzymatic functions by alternating the hydrogen bond network. This mutual interaction subtly alters the function of protein and ultimately determines the form of life [13]. However, protein-water interaction is probably the least understood one among all the important problems in chemical biology. Protein dynamics involve many characteristic events of which the time scales cover a wide range. This complexity poses a challenge to the analysis of experimental data. A series of spectroscopic methods, such as X-ray crystallography [14–18], nuclear overhauser effect NMR [19–21], elastic/inelastic neutron scattering [22–25], NMR dispersion [26–29], time resolved fluorescence [30–36], TeraHerz spectroscopy [37, 38], infrared spectroscopy [39–41], and optical Kerr-effect [42–44] have been developed to date to scrutinize the protein dynamics on a wide range of time scales. Unfortunately, these experiments give contradictory points of view. For instance, using the intrinsic tryptophan (TRP) as a local optical probe [45–49], Li observed the relaxation time scales to be 5 ps and 87 ps by ultrafast fluorescence study of the mutated myoglobin. They suggested that the initial dynamics and slow relaxation are related to fast local motions and strongly coupled water-

Published online: 27 March 2014

protein motions [50]. While, NMR studies revealed that the lifetime is within the sub-nanosecond regime [51, 52]. Competition of fluorescence with other dark processes adds more difficulties to the interpretation of spectrum [53, 54].

Computational investigation of protein dynamics is now routinely utilized to peel down different characteristic motions, due to its strength in high spatiotemporal resolution. However, its participation has not reconciled the contradiction [55–61]. Instead, it adds more controversy to this debate. Theoretical studies predicted that there is an ultrafast decay of the fluorescence at the time scale of tens to a hundred of femtoseconds, which is missing in experimental measurements. There is a significant discrepancy existing between experiment and theory, which raises a serious issue of the traditional force fields used in simulations or the interpretations of the experimental spectra. This conflict is likely due to the low resolution of experimental instruments relative to molecular dynamics simulation. However, a recent study by Zhong's group suggested that the missing percentage could be minor when the solvation dynamics is on the similar time scale as the temporal resolution, and pushed the integrity of the force field to the issue [62]. The reliability of computer simulation depends on the accuracy of the potential energy used to represent the interactions within protein and between protein and solvent molecules. Lack of explicit polarization effect has been known as the dominant limitation of some contemporary force fields such as AMBER, CHARMM, and OPLS. In these force fields, the atomic charges are only the effective charge, of which the parameters are calibrated to absorb the polarization energy term in a pairwise interaction framework [63–65]. Therefore, it is valuable to employ the explicit polarization effect in molecular dynamics simulations and study its impact on the simulated characteristic time scales of protein and water motions. We have shown that with polarized charge for protein and water molecules in the first solvation shell, the average life time of protein/water hydrogen bonds increases, and the structure of water molecules in the first solvation shell is less labile than that under unpolarized charge model [66]. In the past decade, much progress has been achieved in the development of polarizable force fields. Fluctuation charge, Drude-oscillator and induced multipoles have been well parameterized and coded into several molecular dynamics package such as AMBER, CHARMM, and Tinker [67–77]. Realization of these polarization models opens a new era of molecule modeling.

In this work, we studied the hydration dynamics of myoglobin (Mb) with both AMBER force field and the polarized protein-specific charges (PPC) [78] in the framework of linear response. In pairwise force fields, polarization is counted in a homogeneous way, which is not enough to give an adequate delineation of the heterogeneous charge distribution in protein. PPC is designed to give a picture of charge distribution in high fidelity for protein. It is fitted from on-site quantum mechanical calculation for each residue. It captures the specific electrostatic environment intrinsically. Comparing the results from simulations employing unpolarized AMBER charge and PPC, we can tell the impact of polarization effect on the simulated thermal motion of protein in water. We also utilized a recently developed AMBER12pol force field in the simulation in order to confirm the conclusion.

Computational method

Simulations

The initial structure of myoglobin (PDB: 1MBD) was taken from the Protein Data Bank. Heme group was removed. Myoglobin has 153 amino acids [79] aligned into eight α -helices embracing a hydrophobic core. It contains two intrinsic tryptophan residues, i.e., Trp7 and Trp14, which are both located in the α -helix near the N-terminal. Trp14 is buried inside the hydrophobic core, while Trp7 is exposed to the solvent and is more slaved by water molecules [80]. We chose Trp7 as the probe to study the characteristic time scales of thermal motion. The protein was solvated in a TIP3P water box with the minimal distance between the protein and the boundary of the box no less than 12 Å. There were altogether 9362 water molecules. Two chlorine ions were added to neutralize the system. The system was optimized by 180,000 steps steepest descent minimization to remove bad contact, followed by conjugate gradient minimization until convergence was reached. The Coulomb interaction was calculated by using the particle mesh Ewald (PME) algorithm with a cutoff of 10 Å in real space and van der Waals interaction was truncated at 10 Å. The system was heated up from 0 to 300 K in 100 ps with weak restraint applied to the protein. In the relaxation stage, a 100 ns simulation was conducted with a time step of 2 fs. The trajectories were saved every 500 steps (1 ps). This length is long enough to investigate the stability of protein under these force fields. However, a frequency of 1 ps^{-1} for recording the conformations is not enough for visualizing the ultrafast motion patterns on fs time scale. Therefore, we ran another 2.5 ns simulation for each force field and the trajectories were saved every 20 fs. Pairwise AMBER99SB force field, PPC and AMBER12pol force field were utilized. Three versions of PPC were fitted and employed in the simulations, which differed in the implementation of solvation effect while fitting the charge. In the first version, an implicit solvent model was utilized, and induced charges on the solute-solvent interface, which polarized the electronic structure of protein, were calculated by solving the Poisson-Boltzmann equation. In the other two versions, some of the solvent molecules were explicitly included as background charges to polarize the electronic structure of the protein. In the fitting of the second version of PPC (denoted

as PPC′), water molecules in the first solvent shell also have their atomic charges fitted, just like the residues in the protein. Water molecules in a larger shell (5.5 Å) were included in the fitting of the third version of PPC (denoted as PPC″). Atomic charges were fitted residue-by-residue with the restrained electrostatic potential (RESP) method [81, 82]. Electrostatic potential around each residue was calculated at B3LYP/6-31G* level utilizing a molecular tailoring approach termed molecular fractionation with conjugate caps (MFCC) [83, 84]. Polarization among residues and from solvent molecules were included in the quantum mechanical calculations as background charges. Restraints were applied to maintain the total atomic charge of each residue to be an integer, therefore charge flow among residues was not allowed. In the simulation with AMBER12pol force field, POL3 water model was utilized instead of the unpolarizable TIP3P water model. Due to the slow convergence of the correlation of the interaction energy, the simulation employing AMBER12pol force field extended to 3.5 ns. All the simulations were carried out by AMBER12 package.

Atomic charge of Trp7 at the excited state

We assumed that the excitation of Trp7 was localized on the indole ring, which did not depend on its chemical environment. Strictly, this assumption does not hold, but we think that it does not significantly affect the conclusion of this study. Therefore, we calculated the charge distributions of an indole ring in the ground state and the excited state instead of Trp. Electronic structures of its ground state and L_a excited state [85–88] were calculated by time-dependent density functional theory [89–91] at PBEPBE/6-31+G* level in gas phase. ESP charge was fitted for the ground state and the excited state utilizing their electron densities accordingly. Redistributed charge within the indole ring after excitation was added to AMBER charge or PPC of TRP7 for the MM simulations at the excited state. All the quantum mechanical calculations were carried out with Gaussian 09 package [92].

Linear response theory

Although the physical nature of photo excitation and fluorescence emission is a non-equilibrium process, fluctuation-dissipation theory indicates that equilibrium simulation can provide approximately the same information [93, 94]. Linear response is a good approximation in the study of solvation dynamics in polar solvents. However, dielectric response of protein is far more complicated. Even so, the linear response theory is still widely used in the interpretation of the time-dependent Stokes shift (TDSS) of optical probes 'solvated' in proteins. [11, 95–100]. In linear response theory, the characteristic time scales for TDSS are extracted from the time correlation function $C(t)$ of energy gap between the excited state and the ground state, which is calculated as

$$C(t) = \frac{< \Delta E(t)\Delta E(0) > - < \Delta E(0) >^2}{< \Delta E(0)\Delta E(0) > - < \Delta E(0) >^2}, \quad (1)$$

where $\Delta E(0)$ and $\Delta E(t)$ are the excitation energies at t_0 and t_0+t, respectively. The average is over the different selection of t_0. ΔE was calculated as a sum of the difference in Coulomb interaction energy of TRP7 with its surroundings at the excited state and the ground state and the transition energy in the gas-phase that was almost irrelevant for the calculated Stocks shift.

Results and discussion

Atomic charges in the excited state

The charges used for the indole ring in the ground state and the excited state are shown in Table 1. In our model, these charges result in a dipole moment of 4.16 D and 5.05 D for the ground state and excited state, respectively, under PPC with a difference dipole moment of 2.93 D. As a comparison, we also calculated the ground and excited state dipole moment for AMBER94 charges, which are 2.68 D and 4.36 D respectively. Besides, the directions of the dipoles from PPC are different from those of AMBER99SB force field. The dipole moments of the ground state and the excited state under AMBER94 charge and PPC are shown in Fig. 1.

Table 1 Charges used for the indole ring in the ground state and the excited state

	AMBER99SB		PPC	
Atom	Ground state	Excited state	Ground state	Excited state
CG	−0.1415	0.1952	−0.0983	0.2384
CD1	−0.1638	−0.2705	−0.1841	−0.2908
CD2	0.1243	−0.0028	0.0885	−0.0385
HD1	0.2062	0.1985	0.1966	0.1889
NE1	−0.3418	−0.2106	−0.3204	−0.1892
CE2	0.1380	0.1603	0.1335	0.1558
CE3	−0.2387	−0.2870	−0.1553	−0.2036
HE1	0.3412	0.3460	0.3595	0.3643
CZ2	−0.2601	−0.3662	−0.2236	−0.3297
CZ3	−0.1972	−0.2062	−0.1740	−0.1830
HE3	0.1700	0.1393	0.0892	0.0585
HZ2	0.1572	0.1363	0.1501	0.1292
CH2	−0.1134	−0.1001	−0.1380	−0.1247
HZ3	0.1447	0.1421	0.1283	0.1257
HH2	0.1417	0.1316	0.1253	0.1152
CB	−0.0050	−0.0441	−0.1058	−0.1449

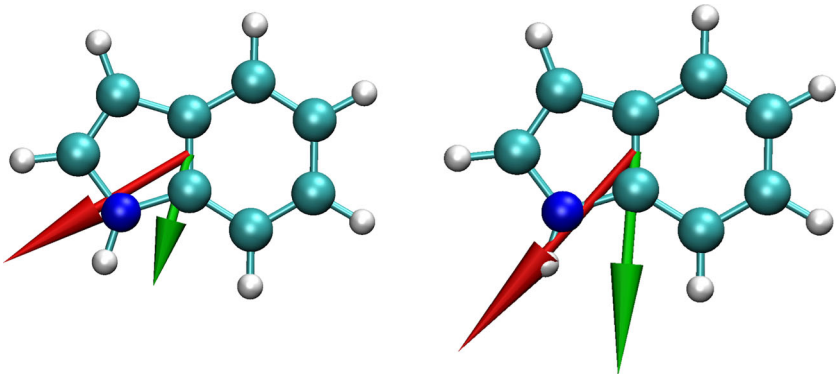

Fig. 1 Dipole moments of the indole ring in the ground state (green) and the excited state (red) under AMBER99SB (left) and PPC (right)

Trajectory stability

Trajectory stability is very important for the simulation of correlation relaxation, otherwise the data would be contaminated by structure drifting. The root mean square deviations (RMSD) from the experimental structure for the backbone atoms in 100 ns simulations employing AMBER99SB force field and PPC respectively are shown in Fig. 2. It is obvious that the backbone RMSD reached a plateau after 30 ns for both AMBER charge and PPC. Under AMBER99SB, the final RMSD is around 2.5 A, which is reasonable for this protein of which the native structure was determined by X-ray diffraction. Under PPC, the RMSD is about 0.5 Å smaller than under AMBER99SB. Therefore, the force fields employed in this work were capable of stabilizing the protein structure, and it was safe to employ these force fields in the following study.

Ultrafast relaxation

As our primary goal was to explore the ultra-fast relaxation of tryptophan interacting with its surroundings and experimental studies had shown that an inertial decay component was on the order of sub-picosecond, we carried out a short simulation in which a total of 125,000 snapshots were saved with 20 fs of time interval. Comparison between AMBER99SB and PPC can tell the impact of internal polarization effect within protein molecule. However, the directional protein-water hydrogen bonds and non-hydrogen bonded protein-water Coulomb interaction have not been fully strengthened. Refitting the atomic charges of the water molecules in the first solvation shell can prolong the life time of protein-water hydrogen bonds [66], which may hamper the relaxation. Therefore, we incorporated 200 water molecules in the first solvation shell into charge fitting. In order to investigate the convergence of relaxation with extending the solvation shell, we also carried out another simulation with water molecules within 5.5 Å from the protein having their atomic charges refitted, as well as the protein. Dynamic properties such as Einstein diffusion constant, rotational diffusion of the water molecules in the first solvation shell, time correlation function are compared to identify how polarization effect impacts the dynamics behavior of protein in water.

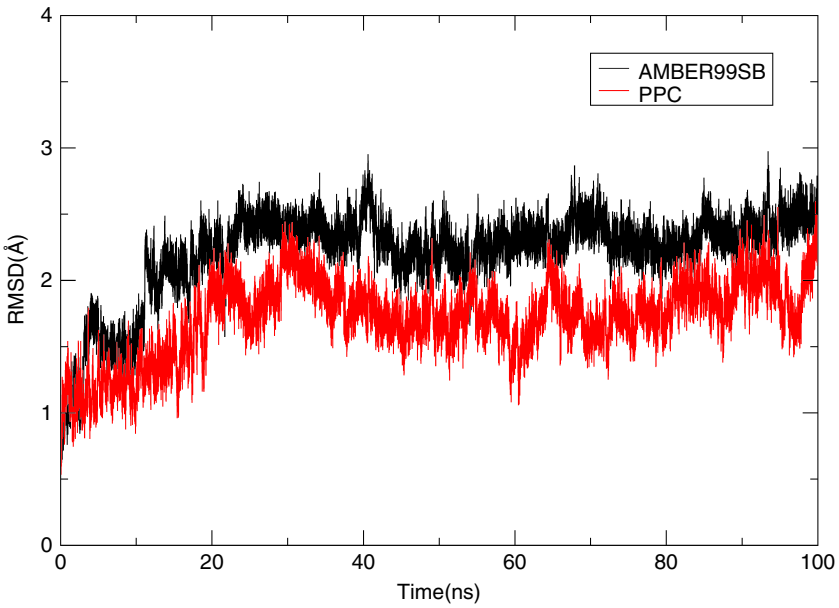

Fig. 2 Root mean square deviation of the backbone atoms from the native structure during the 100-ns simulations utilizing AMBER99SB (black) and PPC (red)

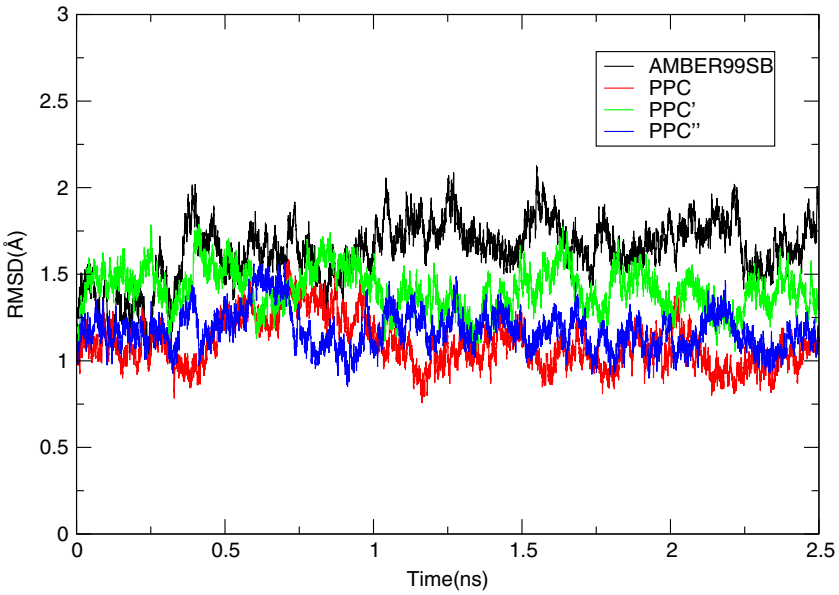

Fig. 3 Root mean square deviations of the backbone atoms in the 2.5 ns equilibrium simulations utilizing AMBER99SB (black), PPC (red), PPC′ (green), and PPC″ (blue)

The time evolutions of the backbone RMSD in all the simulations are shown in Fig. 3. It is consistent with the long time simulations and again it demonstrates that protein is very stable under AMBER99SB and various PPC. The structural stability does not change too much among PPC, PPC′ and PPC″. To get insights into the dynamical behavior of the waters molecules in the first solvation shell of the protein, the Einstein diffusion constant and the rotational diffusion time correlation function for these water molecules were calculated. The Einstein diffusion constants, describing the translational mobility of the solvent molecules, are $0.746\times10^{-9}m^2s^{-1}$, $0.717\times10^{-9}m^2s^{-1}$, $0.615\times10^{-9}m^2s^{-1}$ and $0.579\times10^{-9}m^2s^{-1}$ for AMBER99SB, PPC, PPC′ and PPC″, respectively, indicating that the electrostatic polarization reduces the translational mobility of the solvent molecules. The time correlation functions of the rotational diffusion

$$R(t) = \frac{\langle \boldsymbol{r}(t)\boldsymbol{r}(0)\rangle}{\langle \boldsymbol{r}(0)\boldsymbol{r}(0)\rangle}, \tag{2}$$

for the water molecules in the first solvation shell are depicted in Fig. 4. $\boldsymbol{r}$ is the vector connecting the oxygen atom and the middle point of two hydrogen atoms in each water molecule. The results show that the intra-protein polarization effect can slightly hinder the rotation of the water molecules, and the polarization effect between the protein and the water molecules can further impede the rotational degree-of-freedom of the water molecules.

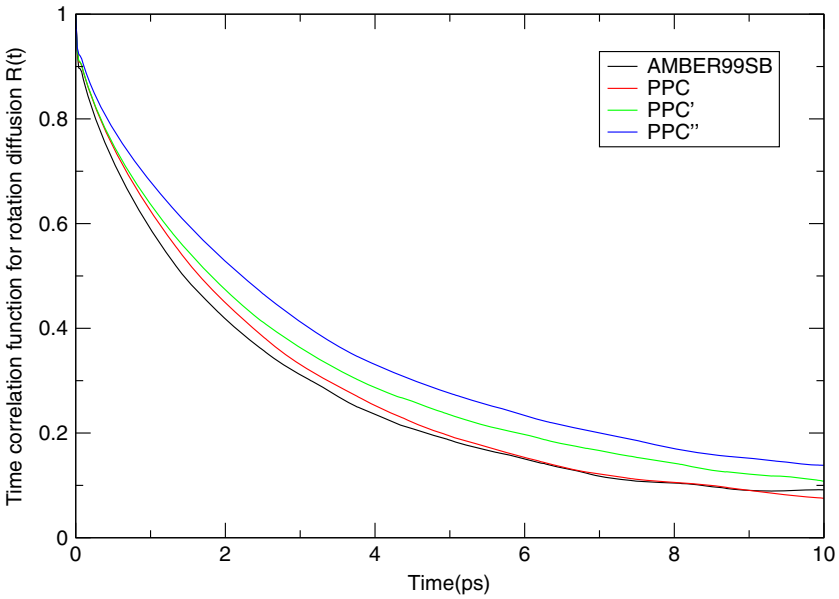

Fig. 4 Rotational time correlation functions of the water molecules in the first solvation shell fitted from the 2.5 ns equilibrium simulations utilizing AMBER99SB (black), PPC (red), PPC′ (green), and PPC″ (blue)

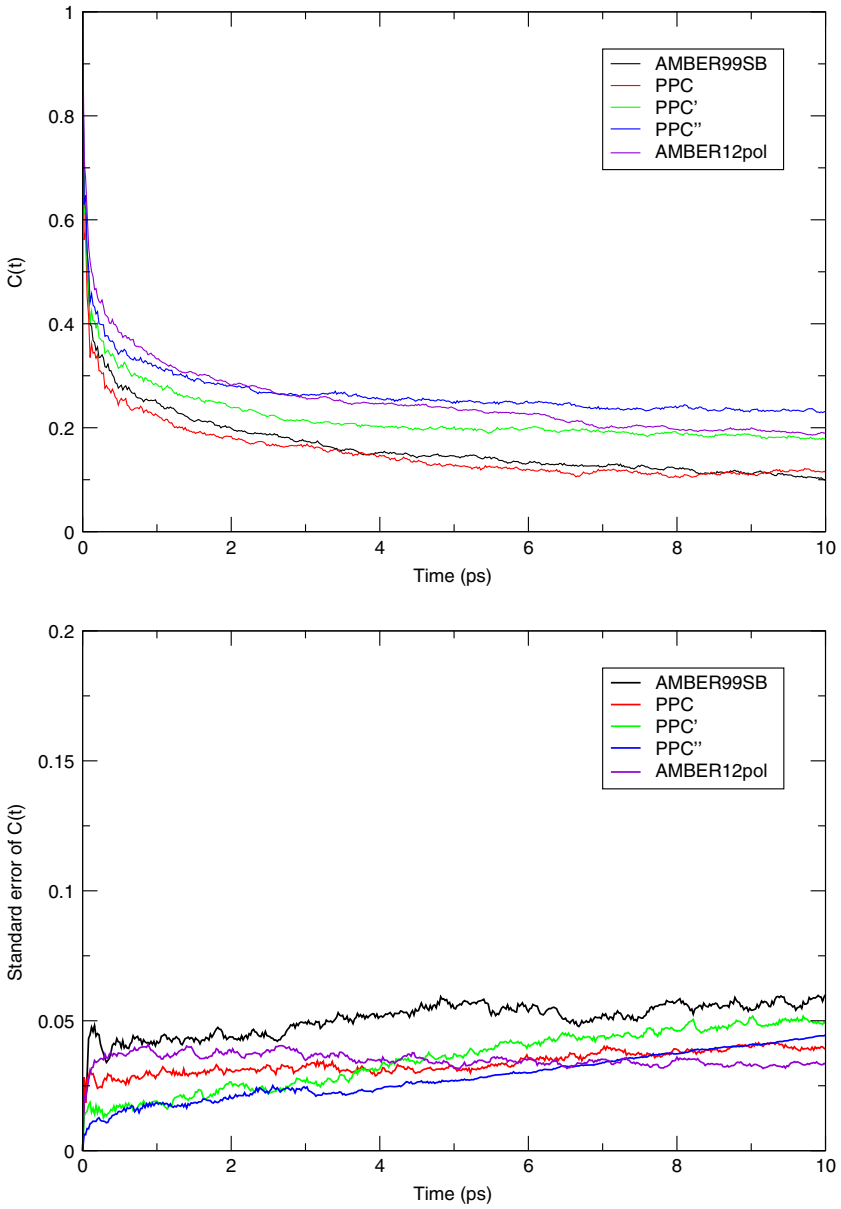

Fig. 5 Relaxation correlation function *C(t)* (top) and its standard deviation (bottom) from the simulations utilizing AMBER99SB (black), PPC (red), PPC′ (green), PPC″ (blue), and AMBER12pol force field (purple)

The Coulomb interaction energies between the indole ring and its environment at the ground and excited states and their difference along the simulation can be calculated straightforwardly. The time correlation function *C(t)* of the difference in Coulomb interaction between the excited state and the ground state is calculated by Eq. 1 and are plotted in Fig. 5. The decays of *C(t)* show clearly a non-exponential fashion. We fit the relaxation curves approximately into tri-exponential functions as

$$C(t) = a_1 * exp(-t/\tau_1) + a_2 * exp(-t/\tau_2) + a3 * exp(-t/\tau_3) \quad (3)$$

with a constraint that the sum of a_i is 1. The characteristic time scale t_1, t_2, and t_3 correspond to the ultrafast, fast, and slow modes of the relaxation, respectively. They can be interpreted as the inertial dynamics, the fast local reorientation/translation motions, and the slow surface hydration dynamics coupled with protein motions [31, 101, 102]. The prefactors a_1, a_2, and

Table 2 The fitted relaxation time scales

	a_1	τ_1 (fs)	a_2	τ_2 (ps)	a_3	τ_3 (ps)
AMBER99SB	0.63	38	0.17	0.95	0.20	15.73
PPC	0.66	32	0.17	1.06	0.17	21.50
PPC′	0.59	31	0.20	0.96	0.21	52.67
PPC″	0.54	30	0.18	0.66	0.28	49.02
AMBER12pol	0.49	37	0.20	0.67	0.31	19.78

a_3 determine how large each motion contributes to the total relaxation relatively. The fitted curves are in high accordance with the calculated time correlation functions with all the correlation coefficient of fitting over 0.99. The fitted parameters for Eq. 3 are shown in Table 2. Under AMBER99SB, the dominant contribution (63 percent) to the relaxation is from the ultrafast motion on femtosecond time scale (38 fs). The fast local motions on 0.95 ps time scale contributes 17 percent of the total relaxation. The other relaxation comes from the slow surface hydration dynamics coupled with protein motions, which has a characteristic time scale of 15.73 ps. When PPC is employed, the intra-protein polarization effect is turned on. However, including this polarization effect only slightly alters the inertial motion. It has only moderate impact on the second time scale by increasing the characteristic time scale by about 12 percent (0.11 ps). Although the longest time scale is lengthened with this intra-protein polarization effect, its contribution to the total relaxation is lowered by 3 percent. Dynamics of protein is slaved by the solvent molecules. According to our previous study, refitting the atomic charges for the water molecules in the first solvation shell leads to strengthened protein-water interaction and the rotational diffusion of the water molecules are hindered [66]. However, the time correlation of the difference in Coulomb interaction energies employing PPC′ does not differ too much from the simulation utilizing AMBER99SB or PPC for the first two relaxation modes. The strong interaction between protein and water molecule can extend further than the first solvation shell and has some impact on the dynamics of the water molecules beyond the first shell. In PPC″ simulation, the water molecules in the second solvation shell are also explicitly polarized. The relaxation as shown in Fig. 5 is slower than those from AMBER99SB, PPC and rmPPC′ simulations, which is originated from the smallest contribution of the initial decay, although its characteristic time scale is comparable. It has the fastest second decay mode, but this mode contributes only 18% to the total relaxation. The pre-exponential factor of its third component is the largest as compared to AMBER99SB, PPC and PPC′, with the time scale a little bit faster than that of PPC′. Therefore, implementation of electrostatic polarization effect cannot fill the gap between the experimental measurement and the theoretical prediction. In order to further confirm our observation, we carried out a simulation employing the recent AMBER polarizable force field. It is shown in Fig. 5 that the initial decay under AMBER12pol force field is a little bit slower than the other force fields. The fitted parameters for Eq. 3 shown in Table 2 indicate that the first characteristic time scale is comparable with those from other force fields, but its contribution to the total relaxation is smaller than the other force fields. The second component is similar to that from PPC″. Its longest time scale is comparable with that from PPC but is much faster than those from PPC′ and PPC″. Its contribution to the total relaxation is just a little bit larger than that from PPC″. From the simulation with AMBER12pol force field, the time scale for the initial relaxation is still much faster than that from the experimental measurement. It confirms the conclusion that the lack of explicit electrostatic polarization effect is not the major cause of the one order gap between the relaxation speeds from simulation and experiment.

Conclusions

The measured ultrafast relaxation time scale for tryptophan in myoglobin is one order slower than the predicted one from molecular dynamics simulations. In this work, we investigate the possibility that employing electrostatic polarization effect can fill the gap through simulations utilizing pairwise AMBER99SB, polarized PPC, and polarizable AMBER12pol force fields. Results show that although employing polarization effect can hinder the rotational and translational motion of water molecules and the relaxation of the tryptophan residue in protein, its impact is very limited and still cannot fill the gap between experiment and theory, at least under linear response approximation. Applicability of linear response approximation has been questioned [103]. More rigorous work such as direct nonequilibrium molecular dynamics simulation at quantum mechanical or quantum mechanical/molecular mechanical hybrid level should be carried out to examine the origin of this gap through rigorous calculations of the possibilities of each possible destination of the excited states, especially the coupling between the indole ring and the carbonyl group. An accurate and fast computational method is in urgent need.

Acknowledgments This work is supported by the National Natural Science Foundation of China (Grant No. 20933002, 21173082 and 11147026) and Shanghai PuJiang program (09PJ1404000). We also thank Supercomputer Center of East China Normal University for CPU time support.

References

1. Jesenska A, Sykora J, Olzynska A, Brezovsky J, Zdrahal Z, Damborsky J, Hof MJ (2009) Am Chem Soc 131:494–501
2. Abbyad P, Shi X, Childs W, McAnaney TB, Cohen BE, Boxer SGJ (2007) Phys Chem B 111:8269–8276
3. Toptygin D, Gronenborn AM, Brand LJ (2006) Phys Chem B 110: 26292–26302
4. Levitt M, Sharon R (1988) Proc Natl Acad Sci U S A 85:7557–7561
5. Lampa-Pastirk S, Beck WFJ (2004) Phys Chem B 108:16288–16294
6. Jordanides XJ, Lang MJ, Song X, Fleming GRJ (1999) Phys Chem B 103:7995–8005
7. Levy Y, Onuchic JN (2006) Annu Rev Biophys Biomol Struct 35: 389–415
8. Pal SK, Zewail AH (2004) Chem Rev 104:2099–2124
9. Bagchi B (2005) Chem Rev 105:3197–3219
10. Bhattacharjee N, Biswas PJ (2011) Phys Chem B 115:12257–12265

11. Bandyopadhyay S, Chakraborty S, Balasubramanian S, Bagchi BJ (2005) Am Chem Soc 127:4071–4075
12. Bandyopadhyay S, Chakraborty S, Bagchi BJ (2005) Am Chem Soc 127:16660–16667
13. Ball P (2008) Chem Rev 108:74–108
14. Srajer V, Ren Z, Teng T-Y, Schmidt M, Ursby T, Bourgeois D, Pradervand C, Schildkamp W, Wulff M, Moffat K (2001) Biochemistry 40:13802–13815
15. Schotte F, Soman J, Olson JS, Wulff N, Anfinrud PAJ (2004) Struct Biol 147:235–246
16. Rejto PA, Freer ST (1996) Prog Biophys Mol Biol 66:167–196
17. Basu RS, Murakami KSJ (2013) Biol Chem 288:3305–3311
18. Srajer V, Royer WE Jr (2008) Time-resolved X-ray crystallography of heme proteins. In: Poole, RK (eds) Globins and other nitric oxide-reactive proteins, part B, vol. 437. Academic, New York, pp 379–395
19. Kay LE (1998) Nat Struct Mol Biol 5:513–517
20. Ishima R, Torchia DA (2000) Nat Struct Mol Biol 7:740–743
21. Hong M, Zhang Y, Hu F (2012) Ann Rev Phys Chem 63:1–24
22. Diehl M, Doster W, Petry W, Schober H (1997) Biophys J 73:2726–2732
23. Zanotti J-M (1999) Bellissent-Funel, M.–C.; Parello, J. Biophys J 76:2390–2411
24. Nickels J, O'Neill H, Hong L, Tyagi M, Ehlers G, Weiss KL, Zhang Q, Yi Z, Mamontov E, Smith JC, Sokolov AP (2012) Biophys J 103:1566–1575
25. Schiro G, Vetri V, Frick B, Militello V, Leone M, Cupane AJ (2012) Phys Chem Lett 3:992–996
26. Kakalis LT, Kumosinski TF (1992) Biophys Chem 43:39–49
27. Orekhov VY, Korzhnev DM, Kay LEJ (2004) Am Chem Soc 126: 1886–1891
28. Morcos F, Chatterjee S, McClendon CL, Brenner PR, Lopez-Rendon R, Zintsmaster J, Ercsey-Ravasz M, Sweet CR, Jacobson MP, Peng JW, Izaguirre JA (2010) PLoS Comput Biol 6:e1001015
29. Xue Y, Ward JM, Yuwen T, Podkorytov IS, Skrynnikov NRJ (2012) Am Chem Soc 134:2555–2562
30. Gardecki JA, Maroncelli MJ (1999) Phys Chem A 103:1187–1197
31. Qiu W, Kao Y-T, Zhang L, Yang Y, Wang L, Stites WE, Zhong D, Zewail AH (2006) Proc Natl Acad Sci U S A 103:13979–13984
32. Zhang L, Wang L, Kao Y-T, Qiu W, Yang Y, Okobiah O, Zhong D (2007) Proc Natl Acad Sci U S A 104:18461–18466
33. Arzhantsev S, Jin H, Baker GA, Maroncelli MJ (2007) Phys Chem B 111:4978–4989
34. Zhang L, Yang Y, Kao Y-T, Wang L, Zhong DJ (2009) Am Chem Soc 131:10677–10691
35. Sajadi M, Obernhuber T, Kovalenko SA, Mosquera M, Dick B, Ernsting NPJ (2009) Phys Chem A 113:44–55
36. Jha SK, Ji M, Gaffney KJ, Boxer SGJ (2012) Phys Chem B 116: 11414–11421
37. Xu J, Plaxco KW, Allen SJ (2006) Protein Sci 15:1175–1181
38. Kim SJ, Born B, Havenith M, Gruebele M (2008) Angew Chem Int Edit 47:6486–6489
39. Arrondo JLR, Goni FM (1999) Prog Biophys Mol Biol 72:367–405
40. Fayer MD (2009) Ann Rev Phys Chem 60:21–38
41. Thielges MC, Axup JY, Wong D, Lee HS, Chung JK, Schultz PG, Fayer MDJ (2011) Phys Chem B 115:11294–11304
42. Giraud G, Wynne KJ (2002) Am Chem Soc 124:12110–12111
43. Hunt NT, Kattner L, Shanks RP, Wynne KJ (2007) Am Chem Soc 129:3168–3172
44. Mazur K, Heisler IA, Meech SRJ (2012) Phys Chem A 116:2678–2685
45. Shen X, Knutson JRJ (2001) Phys Chem B 105:6260–6265
46. Lu W, Kim J, Qiu W, Zhong D (2004) Chem Phys Lett 388:120–126
47. Zhang L, Kao Y-T, Qiu W, Wang L, Zhong DJ (2006) Phys Chem B 110:18097–18103
48. Kim J, Lu W, Qiu W, Wang L, Caffrey M, Zhong DJ (2006) Phys Chem B 110:21994–22000
49. Zhong D, Pal SK, Zhang D, Chan SI, Zewail AH (2002) Proc Natl Acad Sci U S A 99:13–18
50. Li T, Hassanali AA, Kao Y-T, Zhong D, Singer SJJ (2007) Am Chem Soc 129:3376–3382
51. Otting G, Liepinsh E, Wuthrich K (1991) Science 254:974–980
52. Wuthrich K, Billeter M, Guntert P, Luginbuhl P, Riek R, Wider G (1996) Faraday Discuss 103:245–253
53. Vivian JT, Callis PR (2001) Biophys J 80:2093–2109
54. Callis PR, Petrenko A, Muino PL, Tusell JRJ (2007) Phys Chem B 111:10335–10339
55. Steinbach PJ, Brooks BR (1993) Proc Natl Acad Sci U S A 90: 9135–9139
56. Clarage JB, Romo T, Andrews BK, Pettitt BM, Phillips GN (1995) Proc Natl Acad Sci U S A 92:3288–3292
57. Simonson T, Brooks CLJ (1996) Am Chem Soc 118:8452–8458
58. Makarov VA, Andrews BK, Smith PE, Pettitt BM (2000) Biophys J 79:2966–2974
59. Tournier AL, Smith JC (2003) Phys Rev Lett 91:208106
60. Bossa C, Anselmi M, Roccatano D, Amadei A, Vallone B, Brunori M, Di Nola A (2004) Biophys J 86:3855–3862
61. Hassanali AA, Li T, Zhong D, Singer SJJ (2006) Phys Chem B 110: 10497–10508
62. Qin Y, Chang C-W, Wang L, Zhong DJ (2012) Phys Chem B 116: 13320–13330
63. Cerutti DS, Rice JE, Swope WC, Case DAJ (2013) Phys Chem B 117:2328–2338
64. Leontyev IV, Stuchebrukhov AAJ (2010) Chem Theory Comput 6: 3153–3161
65. Karamertzanis PG, Raiteri P, Galindo AJ (2010) Chem Theory Comput 6:1590–1607
66. Gao Y, Guo M, Mei Y, Zhang JZH (2012) Mol Phys 110:595–604
67. Rick SW, Stuart SJ (2003) In Potentials and Algorithms for Incorporating Polarizability in Computer Simulation. Wiley, pp 89–146
68. Wang J, Cieplak P, Li J, Hou T, Luo R, Duan YJ (2011) Phys Chem B 115:3091–3099
69. Wang J, Cieplak P, Li J, Wang J, Cai Q, Hsieh M, Lei H, Luo R, Duan YJ (2011) Phys Chem B 115:3100–3111
70. Wang J, Cieplak P, Cai Q, Hsieh M, Wang J, Duan Y, Luo RJ (2012) Phys Chem B 116:7999–8008
71. Wang J, Cieplak P, Li J, Cai Q, Hsieh M, Luo R, Duan YJ (2012) Phys Chem B 116:7088–7101
72. Ponder JW, Wu C, Ren P, Pande VS, Chodera JD, Schnieders MJ, Haque I, Mobley DL, Lambrecht DS, DiStasio RA, Head-Gordon M, Clark GNI, Johnson ME, Head-Gordon TJ (2010) Phys Chem B 114:2549–2564
73. Shi Y, Xia Z, Zhang J, Best R, Wu C, Ponder JW, Ren PJ (2013) Chem Theory Comput 9:4046–4063
74. Patel S, Brooks CLJ (2004) Comput Chem 25:1–16
75. Patel S, Mackerell AD, Brooks CLJ (2004) Comput Chem 25: 1504–1514
76. Lamoureux G, Roux BJ (2003) Chem Phys 119:3025–3039
77. Lamoureux G, MacKerell AD Jr, Roux BJ (2003) Chem Phys 119: 5185–5197
78. Ji CG, Mei Y, Zhang JZH (2008) Biophys J 95:1080–1088
79. Phillips SE, Schoenborn BP (1981) Nature 292:81–82
80. Stevens JA, Link JJ, Kao Y-T, Zang C, Wang L, Zhong DJ (2010) Phys Chem B 114:1498–1505
81. Bayly CI, Cieplak P, Cornell W, Kollman PAJ (1993) Phys Chem 97:10269–10280
82. Cornell WD, Cieplak P, Bayly CI, Kollmann PAJ (1993) Am Chem Soc 115:9620–9631
83. Zhang DW, Xiang Y, Zhang JZHJ (2003) Phys Chem B 107: 12039–12041
84. W, ZD, H, ZJZ (2003) J Chem Phys 119, 3599
85. Serrano-Andres L, Roos BOJ (1996) Am Chem Soc 118:185–195
86. Sobolewski AL, Domcke W (1999) Chem Phys Lett 315:293–298
87. Callis PR (1997) Methods Enzymol 278:113–150

88. Dedonder-Lardeux C, Jouvet C, Perun S, Sobolewski AL (2003) Phys Chem Chem Phys 5:5118–5126
89. Bauernschmitt R, Ahlrichs R (1996) Chem Phys Lett 256:454–464
90. Casida ME, Jamorski C, Casida KC, Salahub DRJ (1998) Chem Phys 108:4439–4449
91. Furche F, Ahlrichs RJ (2002) Chem Phys 117:7433–7447
92. Frisch MJ, et al (2009) Gaussian 09, Revision B.01
93. Kubo R (1966) Rep Prog Phys 29:255
94. Marconi UMB, Puglisi A, Rondoni L, Vulpiani A (2008) Phys Rep 461:111–195
95. Essiz SG, Coalson RDJ (2009) Phys Chem B 113:10859–10869
96. Lipparini F, Cappelli C, Barone VJ (2012) Chem Theory Comput 8: 4153–4165
97. de Lima GF, Duarte HA, Pliego JRJ (2010) Phys Chem B 114: 15941–15947
98. Coriani S, Fransson T, Christiansen O, Norman PJ (2012) Chem Theory Comput 8:1616–1628
99. Lopata K, Van Kuiken BE, Khalil M, Govind NJ (2012) Chem Theory Comput 8:3284–3292
100. Golosov AA, Karplus MJ (2007) Phys Chem B 111:1482–1490
101. Qiu W, Zhang L, Kao Y-T, Lu W, Li T, Kim J, Sollenberger GM, Wang L, Zhong DJ (2005) Phys Chem B 109:16901–16910
102. Qiu W, Zhang L, Okobiah O, Yang Y, Wang L, Zhong D, Zewail AHJ (2006) Phys Chem B 110:10540–10549
103. Toptygin D, Woolf TB, Brand LJ (2010) Phys Chem B 114: 11323–11337